

Eddy-Currents Computation With T- Ω Discrete Geometric Formulation for an NDE Problem

Ruben Specogna and Francesco Trevisan

Dipartimento di Ingegneria Elettrica, Gestionale e Meccanica, Università of Udine, I-33100 Udine, Italy

We propose a discrete geometric formulation based on a magnetic scalar potential and on the circulation of an electric vector potential to solve eddy-current problems for nondestructive evaluation of steel bars with longitudinal defects.

Index Terms—Discrete formulations, eddy-currents, nondestructive evaluations.

I. INTRODUCTION

WE PRESENT a discrete geometric formulation¹ [1]–[3], for eddy currents based on a magnetic scalar potential Ω and on the circulation T of an electric vector potential associated with nodes and edges of a tetrahedral mesh respectively [4].

With the geometric approach, Maxwell's laws are translated—on a pair of grids one dual of the other— into algebraic equations which hold exactly independently of the size of the mesh. Whereas the discrete counterparts of the constitutive equations—mapping circulations to fluxes or vice versa from one grid to the other—are approximate mesh- and medium-dependent relations. The way in which they are approximated leads to a final stiffness matrix different from the one obtained with the Galerkin approach; a further difference with finite elements stems from the construction of the right-hand side of the final system.

We will apply this formulation to design a device for non-destructive evaluations (NDEs), based on the induction of eddy-currents in a bar with circular cross section, where a thin longitudinal defect is present.

II. DISCRETE GEOMETRIC FORMULATION

We denote with D the domain of interest of our eddy-currents problem. It can be partitioned into a source region D_s , where impressed currents are present, a conductive region D_c and an insulating region $D_a = D - D_s \cup D_c$. We assume linearity of the media and a permeability μ_0 in D and a resistivity ρ in D_c . We introduce in D a pair of interlocked cell complexes² $\tilde{\mathcal{K}}, \mathcal{K}$, Fig. 1. The dual complex $\tilde{\mathcal{K}}$ is simplicial; it consists of *outer* oriented cells such as dual nodes \tilde{n} , dual edges \tilde{e} , dual faces \tilde{f} (triangles), and dual volumes \tilde{v} (tetrahedra).

The primal complex \mathcal{K} is obtained from the dual $\tilde{\mathcal{K}}$ according to the *barycentric* subdivision. It consists of primal nodes n ,

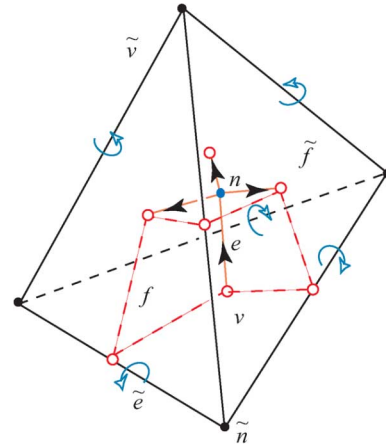


Fig. 1. Representation of the oriented geometric entities forming the pair of the interlocked cell complexes for the case of a single tetrahedron \tilde{v} . The center of mass of \tilde{v} defines the primal node n , and the centers of mass of \tilde{f} and \tilde{e} are denoted with circles. The curved arrowed lines encircling a dual edge \tilde{e} denote the outer orientation of that edge; an arrow denotes the inner orientation of a primal edge e .

edges e , faces f , and volumes v ; for example n coincides with the center of mass of \tilde{v} (Fig. 1).

The mutual interconnections of the dual cell complex $\tilde{\mathcal{K}}$ are described by incidence matrices: $\tilde{\mathbf{G}}$ between dual edges \tilde{e} and dual nodes \tilde{n} , $\tilde{\mathbf{C}}$ between dual faces \tilde{f} and dual edges \tilde{e} , and $\tilde{\mathbf{D}}$ between dual volumes \tilde{v} and dual faces \tilde{f} . The matrices $\mathbf{G} = -\tilde{\mathbf{D}}^T$,³ $\mathbf{C} = \tilde{\mathbf{C}}^T$ and $\mathbf{D} = \tilde{\mathbf{G}}^T$ describe the mutual interconnections of \mathcal{K} .

A. Physical Laws for Eddy-Currents at Discrete Level

We will formulate our eddy-currents problem in terms of arrays of degrees of freedom (DoFs); the DoFs express the integrals of field quantities over the geometric entities of $\tilde{\mathcal{K}}, \mathcal{K}$. The DoFs can be associated in an univocal way to the corresponding geometric entities of $\tilde{\mathcal{K}}$ or \mathcal{K} , [6]. Thus we denote with Φ the array of the induction fluxes on primal faces $f \in D$, with \mathbf{U} the array of e.m.f.s on primal edges $e \in D_c$, with \mathbf{F} the array of m.m.f.s on dual edges $\tilde{e} \in D$ and with \mathbf{I} the array of currents crossing dual faces $\tilde{f} \in D_c \cup D_s$.

We may figure this association introducing the so-called *Tonti diagram* (for a comprehensive description for different physical theories see [7] and [8]). We will briefly retrace the conceptual construction of this diagram, customizing it for our specific

³The minus sign comes from the assumption that n is oriented as a sink, whereas the boundary of \tilde{v} is oriented by the outer normal.

Digital Object Identifier 10.1109/TMAG.2007.916401

Color versions of one or more of the figures in this paper are available online at <http://ieeexplore.ieee.org>.

¹This formulation is part of the geometric approach for Maxwell's equations (GAME) code developed by the authors with the partial support of the Italian Ministry for University and Research (MIUR).

²Informally, in the R^3 ambient space, a cell complex can be understood as a collection of a finite number of geometric entities denoted as *p-cells* like nodes (0-cells), edges (1-cells), faces (2-cells), and volumes (3-cells) endowed with a specific orientation; a precise definition of these concepts can be found in [1], [2], and [6].

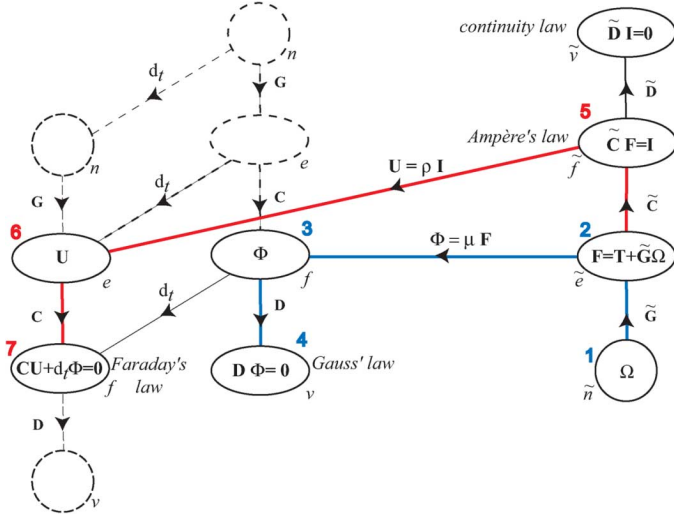


Fig. 2. Tonti's diagram for T-Ω formulation.

eddy-currents formulation. The main advantage of the diagram is to underline the geometric structure behind the Maxwell's equations, and as we will see, it helps in deducing the algebraic system of equations. The diagram should be visualized in a 3-D space, and Fig. 2 gives a perspective view of it. On the left side of the diagram, two vertical pillars are drawn, where each DoF-array, typed inside an oval, is associated with the corresponding geometric entity of the primal cell complex \mathcal{K} (n, e, f, v from top to bottom respectively). On the right side of the diagram, only one vertical pillar is drawn, where each DoF-array, typed inside an oval, is associated with the corresponding geometric element of the dual complex $\tilde{\mathcal{K}}$ ($\tilde{n}, \tilde{e}, \tilde{f}, \tilde{v}$ from bottom to top respectively). The dashed circles represent categories not used in the specific formulation. Along a vertical pillar, we move from the variables associated to a geometric entity to the variables associated with the successive geometric entity, of the primal or of the dual complex, using the incidence matrices. The link between the pair of vertical pillars on the left side of the diagram is given by the time derivative; for a given geometric entity, by taking the time derivative of a DoFs array in the rear pillar, we obtain the corresponding DoFs array in the front pillar. This process allows us to form, for each geometric entity, the physical laws in discrete form. In this way, we may obtain the Maxwell's laws at discrete level, governing an eddy-current problem in the frequency domain. From the left pillars, we deduce Faraday's law as

$$(\mathbf{C}\mathbf{U})_f + i\omega(\Phi)_f = 0 \text{ with } f \in D_c \quad (1)$$

where with symbol $(\mathbf{X})_k$ we mean the k th row of the array \mathbf{X} , k being the label of the corresponding geometric entity, and in this case we set $k = f$. Similarly, from the left rear pillar of the diagram, we deduce the Gauss' Law as

$$(\mathbf{D}\Phi)_v = 0 \text{ with } v \in D. \quad (2)$$

Now, working on the right pillar, Ampère's law becomes

$$(\tilde{\mathbf{C}}\mathbf{F})_{\tilde{f}} = (\mathbf{I})_{\tilde{f}} \text{ with } \tilde{f} \in D_c \cup D_s. \quad (3)$$

For completeness, we add also the continuity law

$$(\tilde{\mathbf{D}}\mathbf{I})_{\tilde{v}} = 0 \text{ with } \tilde{v} \in D_c \cup D_s \quad (4)$$

even though it is implied by the (3), since $\tilde{\mathbf{D}}\tilde{\mathbf{C}} = \mathbf{0}$ holds.

Next, we introduce the array Ω of magnetic scalar potentials Ω associated with the dual nodes $\tilde{n} \in D$ and the array \mathbf{T} of the circulations T of electric vector potential along dual edges $\tilde{e} \in D_c \cup D_s$ such that

$$\begin{aligned} (\mathbf{F})_{\tilde{e}} &= (\tilde{\mathbf{G}}\Omega)_{\tilde{e}} \quad \text{with } \tilde{e} \in D_a \\ (\mathbf{F})_{\tilde{e}} &= (\mathbf{T} + \tilde{\mathbf{G}}\Omega)_{\tilde{e}} \quad \text{with } \tilde{e} \in D_c \cup D_s \end{aligned} \quad (5)$$

hold. However, it is well known that, in the case of multiply connected regions [9], the m.m.f.s along dual edges $\tilde{e} \in D_a$ cannot be described completely by the magnetic scalar potential alone. Therefore, according to the classical approach of the *thick cuts*, we extend the definition of the circulations T of the electric vector potential along the dual edges $\tilde{e} \in D_a$ belonging to the so-called thick cuts regions D_{tc} ; each of these regions is in one-to-one correspondence with primal faces whose collection forms a cut surface. The number of cut surfaces coincides with the number of linearly independent currents in D_c to which correspond an equal number of additional unknown circulations T ; algorithms to compute D_{tc} can be found in [10] and [11].

B. Constitutive Relations

In addition to the physical laws, we need the discrete counterparts of the constitutive relations mapping a DoF array associated with a geometric entity of $\tilde{\mathcal{K}}$ into the dual⁴ geometric entity of \mathcal{K} ; in the diagram, they are represented as horizontal links from right to left. The permeance matrix μ maps the DoF array \mathbf{F} into the DoF array Φ , and we write

$$\Phi = \mu\mathbf{F}. \quad (6)$$

The resistance matrix ρ maps the DoF array \mathbf{I} into the DoF array \mathbf{U} so that

$$\mathbf{U} = \rho\mathbf{I} \quad (7)$$

holds. The permeance and the resistance matrices are some square mesh- and medium-dependent matrices and have dimensions $\dim(\mu) = N_{\tilde{e}}, N_{\tilde{e}}$ being the number of dual edges in D and $\dim(\rho) = N_{\tilde{f}_c}, N_{\tilde{f}_c}$ being the number of dual faces in D_c . These matrices can be constructed according to different techniques described in [4], [5], and [12]; we will dedicate Section IV to construct μ and ρ .

III. ALGEBRAIC SYSTEM

Tonti's diagram is a useful tool to deduce the final system of algebraic equations. We deduce the algebraic system of equations in terms of the Ω and \mathbf{T} arrays, referred to the $\tilde{\mathcal{K}}$ complex only. By substituting (6) and the first of (5), into the (2), we obtain

$$(\mathbf{D}\mu\tilde{\mathbf{G}}\Omega)_{\tilde{n}} = \mathbf{0} \quad \forall \tilde{n} \in D_a - D_{tc} \quad (8)$$

⁴The duality is made evident in the diagram, where the geometric entities on the left and on the right part of the diagram correspond each other; for example $e \leftrightarrow \tilde{f}$ or $f \leftrightarrow \tilde{e}$.

and similarly, substituting (6) and the second of (5) into (2), we obtain

$$(\mathbf{D}\boldsymbol{\mu}\tilde{\mathbf{G}}\boldsymbol{\Omega})_{\tilde{n}} + (\mathbf{D}\boldsymbol{\mu}\mathbf{T})_{\tilde{n}} = \mathbf{0} \quad \forall \tilde{n} \in D_c \cup D_{tc} \cup D_s \quad (9)$$

where $(\mathbf{T})_{\tilde{e}} \forall \tilde{e} \in D_s$ are assigned, and we have that $(\mathbf{T})_{\tilde{e}} = (\mathbf{T}_s)_{\tilde{e}}$ with $\tilde{e} \in D_s$ have prescribed values specified in the array \mathbf{T}_s , related to the source currents in D_s . Equations (8) and (9) can be obtained from the diagram by following the path 1-2-3-4 in Fig. 2.

Now, by substituting (7), (6), (3) and the second of (5), into (1), we may write

$$(\mathbf{C}\boldsymbol{\rho}\tilde{\mathbf{C}}\mathbf{T})_{\tilde{e}} + i\omega\boldsymbol{\mu}(\mathbf{T} + \tilde{\mathbf{G}}\boldsymbol{\Omega})_{\tilde{e}} = \mathbf{0} \quad \forall \tilde{e} \in D_c. \quad (10)$$

This equation can be obtained from the diagram following the paths 2-5-6-7 and 2-3-7 in Fig. 2.

Finally, since to each thick cut domain in D_{tc} corresponds an additional unknown T , we need as many additional equations as the number of the thick cut domains. Each of these additional equations is deduced from (1) applied to the cut surface and to its boundary respectively. To close the problem, we need proper boundary conditions on dual nodes and edges on ∂D and interface conditions on ∂D_c .

A. Integral Representation of Sources

In order to avoid the specification of the array \mathbf{T}_s in (9), we adopt an integral representation of the effect of the source currents in D_s . Thanks to the linearity of media, we can express the DoF array \mathbf{F} of m.m.f.s along dual edges as $\mathbf{F} = \mathbf{F}_s + \mathbf{F}_c$ where \mathbf{F}_s is the array of m.m.f.s produced by the source currents in D_s and \mathbf{F}_c is the array of m.m.f.s due to the eddy-currents in D_c . Each entry F_s of the array \mathbf{F}_s can be computed as $F_s = \int_{\tilde{e}} \mathbf{H}_s \cdot d\mathbf{l}$, where \mathbf{H}_s is the magnetic field expressed by the Biot-Savart law from the source currents in D_s and \tilde{e} is a dual edge. Applying (3) to \mathbf{F}_s , the following properties hold: $(\tilde{\mathbf{C}}\mathbf{F}_s)_{\tilde{f}} = (\mathbf{I}_s)_{\tilde{f}} \forall \tilde{f} \in D_s$, where \mathbf{I}_s is the array of source currents indexed over the dual faces in D_s ; moreover $(\tilde{\mathbf{C}}\mathbf{F}_s)_{\tilde{f}} = 0$ holds $\forall \tilde{f} \in D - D_s$.

Similarly $(\tilde{\mathbf{C}}\mathbf{F}_c)_{\tilde{f}} = (\mathbf{I}_c)_{\tilde{f}} \forall \tilde{f} \in D_c$ holds, where \mathbf{I}_c is the array of the eddy currents in D_c ; moreover $(\tilde{\mathbf{C}}\mathbf{F}_c)_{\tilde{f}} = 0 \forall \tilde{f} \in D - D_c$ holds.

Next, since relations (5) hold also for \mathbf{F}_c , we may write $(\mathbf{F}_c)_{\tilde{e}} = (\tilde{\mathbf{G}}\boldsymbol{\Omega})_{\tilde{e}}$ with $\tilde{e} \in D_a - D_{tc}$ and $(\mathbf{F}_c)_{\tilde{e}} = (\mathbf{T}_c + \tilde{\mathbf{G}}\boldsymbol{\Omega})_{\tilde{e}}$ with $\tilde{e} \in D_c \cup D_s \cup D_{tc}$, where \mathbf{T}_c is the array of the circulation of the electric vector potential due to the eddy currents in D_c . Therefore (8), (9), and (10) can be rewritten respectively as

$$\begin{aligned} (\mathbf{D}\boldsymbol{\mu}\tilde{\mathbf{G}}\boldsymbol{\Omega})_{\tilde{n}} &= -(\mathbf{D}\boldsymbol{\mu}\mathbf{F}_s)_{\tilde{n}} \quad \forall \tilde{n} \in D_a - D_{tc} \\ (\mathbf{D}\boldsymbol{\mu}\tilde{\mathbf{G}}\boldsymbol{\Omega})_{\tilde{n}} + (\mathbf{D}\boldsymbol{\mu}\mathbf{T}_c)_{\tilde{n}} &= -(\mathbf{D}\boldsymbol{\mu}\mathbf{F}_s)_{\tilde{n}} \\ &\quad \forall \tilde{n} \in D_c \cup D_{tc} \cup D_s \\ (\mathbf{C}\boldsymbol{\rho}\tilde{\mathbf{C}}\mathbf{T}_c)_{\tilde{e}} + i\omega\boldsymbol{\mu}(\mathbf{T}_c + \tilde{\mathbf{G}}\boldsymbol{\Omega})_{\tilde{e}} &= -i\omega(\boldsymbol{\mu}\mathbf{F}_s)_{\tilde{e}} \quad \forall \tilde{e} \in D_c. \end{aligned} \quad (11)$$

IV. CONSTRUCTION OF THE CONSTITUTIVE MATRICES

To construct the permeance $\boldsymbol{\mu}$ and resistance $\boldsymbol{\rho}$ constitutive matrices we will resort to the edge and face vector base functions defined in [5], [13], and [14] within a different geometric

context. Therefore, we will recall briefly their geometric construction tailoring them to the specific geometry of our cell complexes \mathcal{K} , $\tilde{\mathcal{K}}$. As proven in the above-cited papers, these base functions assure that symmetry, positive-definiteness, and consistency⁵ properties are satisfied for both the matrices $\boldsymbol{\mu}$, $\boldsymbol{\rho}$. To construct $\boldsymbol{\mu}$, $\boldsymbol{\rho}$ we will refer to a single tetrahedron \tilde{v} with a uniform permeability μ or resistivity ρ ; the constitutive matrices for the overall mesh of tetrahedra are obtained by summing up the contributions from the single elements. We will denote with \tilde{n} the four dual nodes of tetrahedron \tilde{v} and with v the four primal volumes in \tilde{v} ; each v is a hexahedron in a one-to-one correspondence with a node \tilde{n} , Fig. 1. We denote with V the volume of \tilde{v} .

A. Resistance Constitutive Matrix

The entries of matrix $\boldsymbol{\rho}$, of dimension 4×4 for tetrahedron \tilde{v} are computed as

$$\rho_{ij} = \int_{\tilde{v}} \mathbf{v}_{\tilde{f}_i} \cdot \rho \mathbf{v}_{\tilde{f}_j} dv \quad (12)$$

where $\mathbf{v}_{\tilde{f}_i}$ is the face vector function associated with the dual face \tilde{f}_i of tetrahedron \tilde{v} ; the nodes of the face \tilde{f}_i are denoted by $\tilde{n}_a, \tilde{n}_b, \tilde{n}_c$ respectively. The support of $\mathbf{v}_{\tilde{f}_i}$ is the union of the three primal volumes having a nonnull intersection with face \tilde{f}_i ; we denote these primal volumes as v_a, v_b, v_c and the corresponding dual nodes as $\tilde{n}_a, \tilde{n}_b, \tilde{n}_c$ respectively. We also denote with $\tilde{e}_r, \tilde{e}_s, \tilde{e}_t$ the edge vectors associated with edges $\tilde{e}_r, \tilde{e}_s, \tilde{e}_t$ drawn from the nodes $\tilde{n}_a, \tilde{n}_b, \tilde{n}_c$ and not belonging to the boundary of \tilde{f}_i .

Then, the face vector function $\mathbf{v}_{\tilde{f}_i}$ attached to \tilde{f}_i is defined as

$$\mathbf{v}_{\tilde{f}_i}(p) = \begin{cases} \tilde{D}_{\tilde{v}i} \tilde{G}_{ra} \frac{\tilde{e}_r}{3\tilde{V}}, & \text{if } p \in v_a \\ \tilde{D}_{\tilde{v}i} \tilde{G}_{sb} \frac{\tilde{e}_s}{3\tilde{V}}, & \text{if } p \in v_b \\ \tilde{D}_{\tilde{v}i} \tilde{G}_{tc} \frac{\tilde{e}_t}{3\tilde{V}}, & \text{if } p \in v_c \end{cases} \quad (13)$$

where $\tilde{D}_{\tilde{v}i}$ is the incidence number between outer orientations of the pair \tilde{v} and \tilde{f}_i ; \tilde{G}_{ra} is the incidence number between outer orientations of the pair \tilde{e}_r, \tilde{n}_a and similarly for the others.

B. Permeance Constitutive Matrix

The entries of matrix $\boldsymbol{\mu}$, of dimension 6×6 for tetrahedron \tilde{v} , are computed as

$$\mu_{ij} = \int_{\tilde{v}} \mathbf{v}_{\tilde{e}_i} \cdot \mu \mathbf{v}_{\tilde{e}_j} dv \quad (14)$$

where $\mathbf{v}_{\tilde{e}_i}$ is the edge vector function associated with the dual edge \tilde{e}_i of tetrahedron \tilde{v} ; the nodes of the edge \tilde{e}_i are denoted by \tilde{n}_a, \tilde{n}_b respectively. The support of $\mathbf{v}_{\tilde{e}_i}$ is the union of the two primal volumes having a nonnull intersection with edge \tilde{e}_i ; we denote these primal volumes as v_a, v_b and the corresponding dual nodes as \tilde{n}_a, \tilde{n}_b respectively. We also denote with \tilde{f}_r, \tilde{f}_s the

⁵A precise definition of the notion of consistency for constitutive matrices is given in [2].

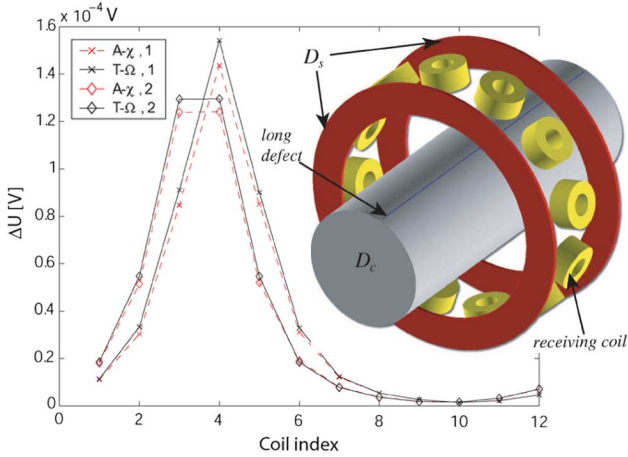


Fig. 3. (Left) Voltage variation versus the receiving coil index (from 1 to 12) for different relative angular locations between the coils and the defect (with label 1 the defect is under coil 4, with the label 2 the defect is located between coils 3 and 4). (Right) The conducting bar D_c , the pair of source coils D_s , and the array of receiving coils are shown.

face vectors⁶ associated with the faces \tilde{f}_r , \tilde{f}_s . The face \tilde{f}_r has one vertex only coincident with the node \tilde{n}_a , and the face \tilde{f}_s has one vertex only coincident with the node \tilde{n}_b .

Then, the edge vector function $v_{\tilde{e}_i}$ attached to \tilde{e}_i is defined as

$$v_{\tilde{e}_i}(p) = \begin{cases} \tilde{G}_{ia} \tilde{D}_{\tilde{v}_r} \frac{\tilde{f}_r}{3V}, & \text{if } p \in v_a \\ \tilde{G}_{ib} \tilde{D}_{\tilde{v}_s} \frac{\tilde{f}_s}{3V}, & \text{if } p \in v_b \end{cases} \quad (15)$$

where \tilde{G}_{ia} is the incidence number between \tilde{e}_i and \tilde{n}_a , and $\tilde{D}_{\tilde{v}_r}$ is the incidence number between \tilde{v} and \tilde{f}_r .

V. APPLICATION AND RESULTS

The application concerns the design of a device for the detection of long longitudinal defects that can be present during the hot mill rolling process of the steel bars with circular cross-section. The bar consists of a conducting AISI 310 steel cylinder (34 mm of diameter and conductivity of $1.236 \cdot 10^6$ S/m), where a longitudinal perfectly insulating defect is assumed, 0.5 mm deep from the surface of the cylinder and 0.2 mm thick. A pair of source coils (30 mm of inner radius, 39 mm of outer radius, 1 mm height, 7 turns each, $I = 200$ mA per turn, $f = 100$ kHz, counter series connected, 30 mm of axial distance between the coils) encircling the bar are considered as sources. A set of 12 evenly spaced circular coils (3 mm of inner radius, 6.5 mm outer radius, 6 mm height, 400 turns) with axis directed as the radii of the bar are considered in between the pair of source coils.

When detecting long defects, a reference signal for each coil is not available, and therefore it is not possible to use a differential detection system. To detect the defect we use an inversion technique based on a neural network.

To have an estimate of the expected voltage variations in the coils due to the presence of the defect, we computed the voltage variations $\Delta U = U_d - U_0$ between the voltage on each coil U_d when the defect is present and the voltage U_0 on the same coil without the defect.

To this aim we need to solve a pair of eddy-currents problems; we used the GAME code with the $T - \Omega$ formulation and

integral representation of sources (11). The mesh used consists of about 218 000 tetrahedrons, 257 000 edges and 37 629 nodes. The defect has been modeled as a volume discretized with a collection of tetrahedra. The results, compared with an independent $A - \chi$ formulation [12], are shown in Fig. 3 together with the geometry of the problem. The time to solve each linear system, obtained from the same mesh of tetrahedra, on a Pentium IV 3-GHz laptop, 2-GB RAM, is 126 s for the $T - \Omega$ formulation, while the $A - \chi$ formulation takes 176 s.

VI. CONCLUSION

We presented a discrete geometric formulation for the solution of eddy-currents problems based on a magnetic scalar potential on dual nodes and on the circulation of the electric vector potential on dual edges. The constitutive matrices are constructed geometrically in such a way that consistency and stability are guaranteed. The numerical code has been used to design a device for the detection of long longitudinal defects in circular bars. The computed voltage variations on the receiving coils for different relative positions of the defect, are in a very good agreement with those from an independent formulation $A - \chi$ previously developed.

REFERENCES

- [1] A. Bossavit, "How weak is the weak solution in finite elements methods?," *IEEE Trans. Magn.*, vol. 34, no. 5, pp. 2429–2432, 1998.
- [2] A. Bossavit and L. Kettunen, "Yee-like schemes on staggered cellular grids: A synthesis between FIT and FEM approaches," *IEEE Trans. Magn.*, vol. 36, no. 4, pp. 861–867, 2000.
- [3] E. Tonti, "Finite formulation of the electromagnetic field," *IEEE Trans. Magn.*, vol. 38, no. 2, pp. 333–336, 2002.
- [4] F. Trevisan and L. Kettunen, "Geometric interpretation of finite dimensional eddy current formulations," *Int. J. Numer. Methods Eng.*, vol. 67, no. 13, pp. 1888–1908, 2006.
- [5] L. Codecasa and F. Trevisan, "Piecewise uniform bases and energetic approach for discrete constitutive matrices in electromagnetic problems," *Int. J. Numer. Methods Eng.*, vol. 65, no. 4, pp. 548–565, 2006.
- [6] E. Tonti, "Algebraic topology and computational electromagnetism," in *Proc. 4th Int. Workshop on Electric and Magnetic Fields*, Marseille, France, May 12–15, 1988, pp. 284–294.
- [7] E. Tonti, "On the formal structure of physical theories," *Quaderni dei Gruppi di Ricerca Matematica del CNR*, 1975.
- [8] E. Tonti, "On the geometrical structure of electromagnetism," in *Gravitation, Electromagnetism and Geometrical Structures for the 80th Birthday of A. Lichnerowicz*, G. Ferrarese, Ed. Bologna, Italy: Pitagora Editrice, 1995, pp. 281–308.
- [9] L. Kettunen, K. Forsman, and A. Bossavit, "Formulation of the eddy current problem in multiply connected regions in terms of h ," *Int. J. Numer. Meth. Eng.*, vol. 41, no. 5, pp. 935–954, 1998.
- [10] P. W. Gross and P. R. Kotiuga, *Electromagnetic Theory and Computation: A Topological Approach*. Cambridge, U.K.: Cambridge Univ. Press, 2004, vol. 48.
- [11] S. Suuriniemi, "Homologicam computations in electromagnetic modeling," Ph.D. thesis, Tampere Univ. Technol., Tampere, Finland, 2004.
- [12] R. Specogna and F. Trevisan, "Discrete constitutive equations in $A - \chi$ geometric eddy-current formulation," *IEEE Trans. Magn.*, vol. 41, no. 4, pp. 1259–1263, 2005.
- [13] L. Codecasa, R. Specogna, and F. Trevisan, "Symmetric positive-definite constitutive matrices for discrete eddy-current problems," *IEEE Trans. Magn.*, vol. 42, no. 2, pp. 510–515, 2007.
- [14] L. Codecasa, V. Minerva, and M. Politi, "Use of barycentric dual grids for the solution of frequency domain problems by FIT," *IEEE Trans. Magn.*, vol. 40, no. 2, pp. 1414–1419, 2004.

⁶This is a vector normal to the face oriented as the outer orientation of the face and with amplitude equal to the area of the face.